ELSEVIER

Biochimica et Biophysica Acta 1609 (2003) 19–27

BIOCHIMICA ET BIOPHYSICA ACTA
BBA

www.bba-direct.com

Review

β-Barrel membrane protein folding and structure viewed through the lens of α-hemolysin

Michelle Montoya[a,*], Eric Gouaux[a,b,*]

[a] *Department of Biochemistry and Molecular Biophysics, Columbia University, New York, NY 10032, USA*
[b] *Howard Hughes Medical Institute, Columbia University, New York, NY 10032, USA*

Received 12 September 2002; received in revised form 12 November 2002; accepted 14 November 2002

Abstract

The β-barrel is a transmembrane structural motif commonly encountered in bacterial outer membrane proteins and pore-forming toxins (PFTs). α-Hemolysin (αHL) is a cytotoxin secreted by *Staphylococcus aureus* that assembles from a water-soluble monomer to form a membrane-bound heptameric β-barrel on the surface of susceptible cells, perforating the cell membranes, leading to cell death and lysis. The mechanism of heptamer assembly, which has been studied extensively, occurs in a stepwise manner, and the structures of the initial, monomeric form and final, membrane-embedded pore are known. The toxin's ability to assemble from an aqueous, hydrophilic species to a membrane-inserted oligomer is of interest in understanding the assembly of PFTs in particular and the folding and structure of β-barrel membrane proteins in general. Here we review the structures of the monomeric and heptamer states of LukF and αHL, respectively, the mechanism of toxin assembly, and the relationships between αHL and nontoxin β-barrel membrane proteins.

Keywords: β-Barrel; Protein folding; α-Hemolysin

There are two structural classes of transmembrane proteins: α-helical and β-barrel. The α-helical motif is most often found in the receptors and ion channels of plasma and endoplasmic reticulum membranes. Information about the folding of α-helical membrane proteins has largely been provided from studies of bacteriorhodopsin (reviewed in Ref. [1]). There is a growing understanding of the folding process in the field of β-barrel membrane protein study, although progress has been slower than with α-helical membrane proteins. The β-barrel is most often encountered in membrane proteins that reside in the outer membrane of Gram-negative bacteria and in the mitochondrial membrane and it is a motif used by many bacterial pore-forming toxins (PFTs) to form cytotoxic transmembrane channels.

PFTs form hydrophilic pores in the cytoplasmic membranes of target cells. These toxins require multiple copies of the protein molecules to form an oligomeric pore. The proteins are released by the bacteria as water-soluble species and subsequently bind to susceptible membranes. Membrane binding increases the local concentration of toxin and triggers conformational changes, thus facilitating the oligomerization process. Toxin oligomerization leads to insertion into the membrane and formation of a protein-lined pore ranging in diameter from 1 to 2 nm for Staphylococcal α-hemolysin (αHL) [2] and *Vibrio cholerae* cytolysin [3], and from 15 to 25 nm for streptolysin O [4] and perfringolysin O [5].

The family of PFTs can be divided into two types: the α-PFTs, which form pores by the insertion of amphipathic α-helices, and the β-PFTs, which form pores by the insertion of amphipathic β-hairpins to create a β-barrel. In both types of PFTs, the hydrophilic side of the protein faces the aqueous environment of the pore while the hydrophobic surface faces the acyl chains of the membrane bilayer. The β-PFTs can be further divided into two subtypes, the first of which forms pores and disrupts cell membranes, compromising cell permeability and leading to cell lysis, as exemplified by αHL; the second subtype consists of the A–B toxins, where the B subunits form oligomeric complexes for

* Corresponding authors. M. Montoya is to be contacted at Fax: +1-212-305-8174. E. Gouaux, Biochemistry and Molecular Biophysics Department, Howard Hughes Medical Institute, Columbia University, 650 West 168th Street, New York, NY 10032, USA. Tel.: +1-212-305-4475; fax: +1-212-305-8174.

E-mail addresses: mm922@columbia.edu (M. Montoya), jeg52@columbia.edu (E. Gouaux).

0005-2736/02/$ - see front matter © 2002 Elsevier Science B.V. All rights reserved.
PII: S0005-2736(02)00663-6

the purpose of delivering the catalytic A portion of the toxin to the cytosol of the target cell, as in the case of the anthrax toxin complex. The A protein moieties of anthrax toxin, lethal factor and edema factor, translocate across endosomal membranes after insertion and pore formation of the B moiety, protective antigen (PA). PA forms homoheptameric

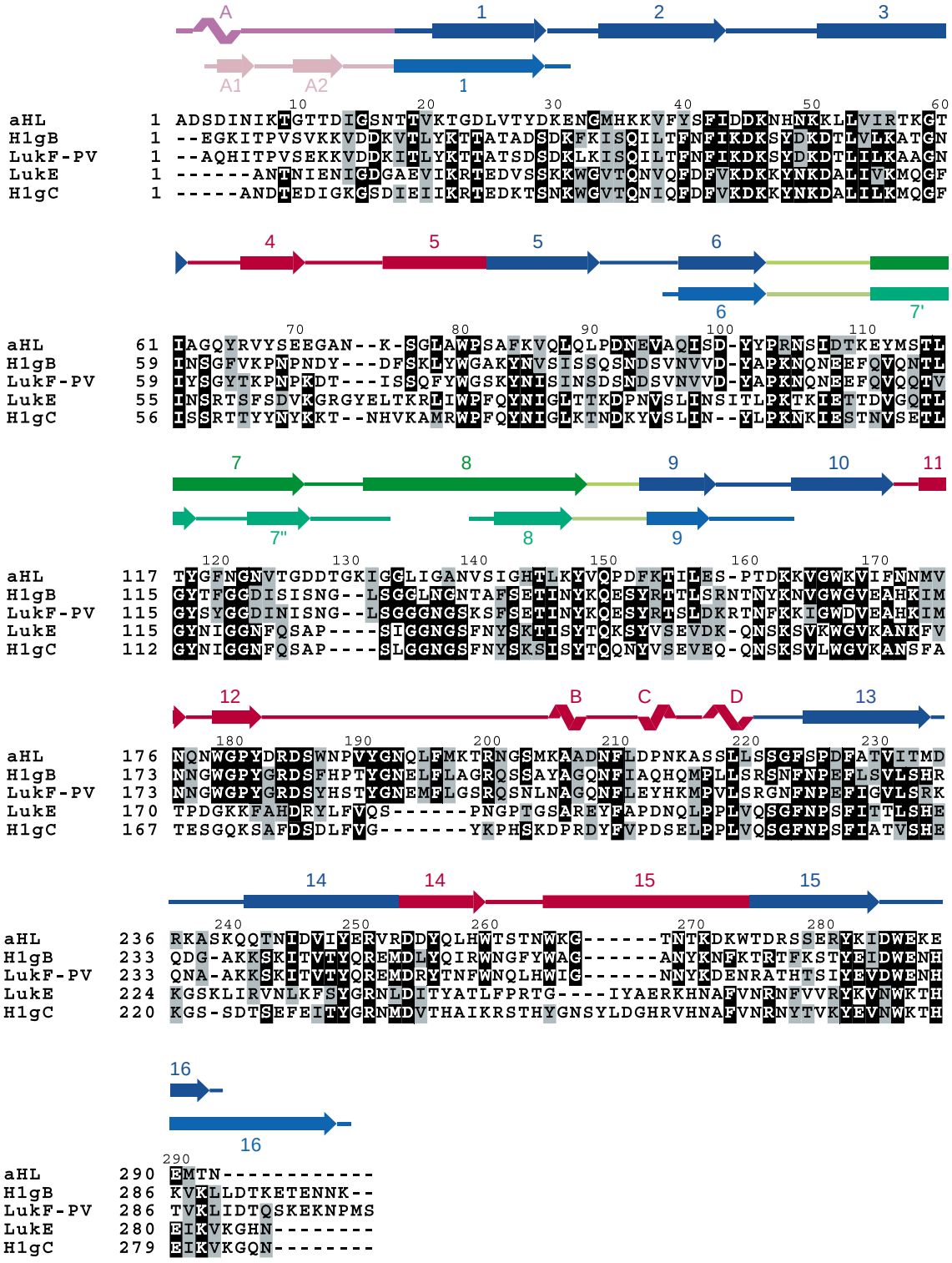

Fig. 1. Alignment of the sequences of αHL, γ-hemolysin (HlgB and HlgC) and Luk (LukF-PV and LukE) proteins. Secondary structure elements of αHL (*upper*) and structural elements unique to the water-soluble, monomeric form of LukF (*lower*) are displayed above the sequences. The sequence numbering is for αHL. Residues with a black background are identical in half or more of the sequences, whereas residues with a grey background are conservative substitutions in half or more of the sequences. ClustalW was used to perform the alignment and Boxshade 3.21 was used to create the figure.

pores [6] composed of a 14-strand β-barrel. A disordered loop present in the water-soluble structure of PA shares sequence characteristics with the pore-forming region of αHL and it has been suggested that the PA pore assembly mechanism is similar to that proposed for αHL [7].

αHL is a β-PFT produced by *Staphylococcus aureus*. Along with the PFTs γ-hemolysin (γHL) and leukocidin (Luk), αHL is one of many toxins secreted by *S. aureus* during the postexponential phase of the bacterium's growth [8,9]. The biologically active state of αHL is a membrane-embedded homoheptameric pore that forms from the assembly of secreted water-soluble monomers on the target cell membrane. Of all the PFTs, it is the best understood structurally, as both endpoints of its assembly process are known.

γHL and Luk are bicomponent β-PFTs related in amino acid sequence and function to αHL [10]. A functional Luk pore is formed from a heterooligomeric complex of class F and class S protomers in ~1:1 ratio [11]. The subunit stoichiometry for Luk is still under debate, with model building and experimental data being marshalled to suggest either heptameric [12] or octameric [13] stoichiometries. There are five classes of F proteins and six classes of S proteins, allowing for 30 possible binary combinations [14]. HγII, a class S subunit, can also combine with class F proteins to form γHL [9]. The F and S proteins are 70% identical within a class, whereas the sequence identity between classes falls to ~30%. The class F proteins are more closely related in sequence to αHL (~30% identity) than the S proteins (~20% identity) (Fig. 1) [15]. Despite the difference in sequence identity, the αHL protomer core is very similar in structure to the class F proteins LukF and LukF-PV [15,16], and, we predict, the remaining class F and class S proteins. αHL and the bicomponent toxins have similar molecular weights and isoelectric points, core hydrophobic residues, and a glycine-rich region located in the middle of the primary sequence [10].

1. Structures

The structure of the heptameric, active form of αHL has been determined in the presence of detergent micelles [17]. Early characterization of the hemolysin oligomer suggested a hexameric subunit stoichiometry [18–21]. Initial crystallographic analysis, in which a seven-fold axis of rotational or screw axis symmetry was discovered [22], suggested that the assembled pore was a heptamer with a seven-fold axis of rotational symmetry. The crystallographic studies, in combination with high-resolution electrophoretic analysis of erythrocyte-assembled toxins, reinforced the conclusion that the αHL oligomer was a heptamer [23]. More recent studies, including atomic force microscopy (AFM) performed on prepore intermediates [24,25] and single-channel conductance experiments using SH modification of an αHL cysteine mutant [26], as well as the crystal structure [17], confirm the heptameric arrangement of the assembled pore. Under some conditions, the results of AFM experiments suggest that αHL oligomers with a hexameric stoichiometry may also be found [27].

The protein complex is mushroom shaped with overall dimensions of 100 Å × 100 Å (Fig. 2). The seven-fold noncrystallographic axis of symmetry runs parallel to the channel opening, which spans the entire length of the protein assemblage. At its widest and narrowest points, the channel diameter is 46 and 14 Å, respectively. The overall architecture of the protein is divided into three domains: the cap, rim and stem. The ca. 48-Å-high cap domain is largely hydrophilic and, with the rim domain, projects from the extracellular surface of the membrane, corresponding to protrusions on lipid membranes viewed by electron microscopy [21]. The cap is composed of seven β sandwiches and amino latches from each protomer. The rim domain lies on the underside of the cap and forms a three-strand β sheet. It is in close proximity and/or direct contact with the outer leaflet of the membrane bilayer. The stem domain is formed by a 14-strand anti-parallel β-barrel, defining the transmembrane portion of the channel. Each protomer contributes two strands to the barrel. The stem is 52 Å high and 26 Å (C_α–C_α) wide.

The protomer core has a kidney-shaped structure that is 70 Å tall along the seven-fold axis and is 45 Å thick and 20 Å wide [17]. An individual protomer consists of a 5+6 β sandwich connected continuously to the rim domain composed of three β strands and non-α, non-β structure, forming the protein core. Two prominent structural features that extend from the core are the amino latch (residues A1–V20), which makes extensive contacts with an adjacent protomer, and the glycine-rich β-strands 7 and 8 (residues K110–Y148), which form the stem domain. The amino latch and glycine-rich stem domains undergo considerable conformational changes during the course of heptamer assembly. The triangle region, formed by residues D103 to T109 and V149 to D152, connects the stem domain to the β-sandwich core. This region participates in key interprotomer interactions in neighboring triangle and rim domains.

The structure of the heptamer revealed, at high resolution, the architecture of the assembled toxin pore. Circular dichroism (CD) experiments showed that the water-soluble monomer and assembled pore had largely β-sheet structures with similar CD spectra, suggesting that there is little change in the net secondary structure composition of the protein during the assembly process [19,20]. Nevertheless, there was abundant evidence to suggest that major conformational changes occurred along the toxin assembly pathway [19,20,28–30]. The crystal structures of the water-soluble form of two class F Luk proteins have helped to elucidate the structural changes occurring as the toxin assembles to form the transmembrane pore.

The structures of the Luk F component HlgB (LukF) and the Panton-Valentine Luk F component (LukF-PV) have been determined [15,16]. The amino acid sequences of these

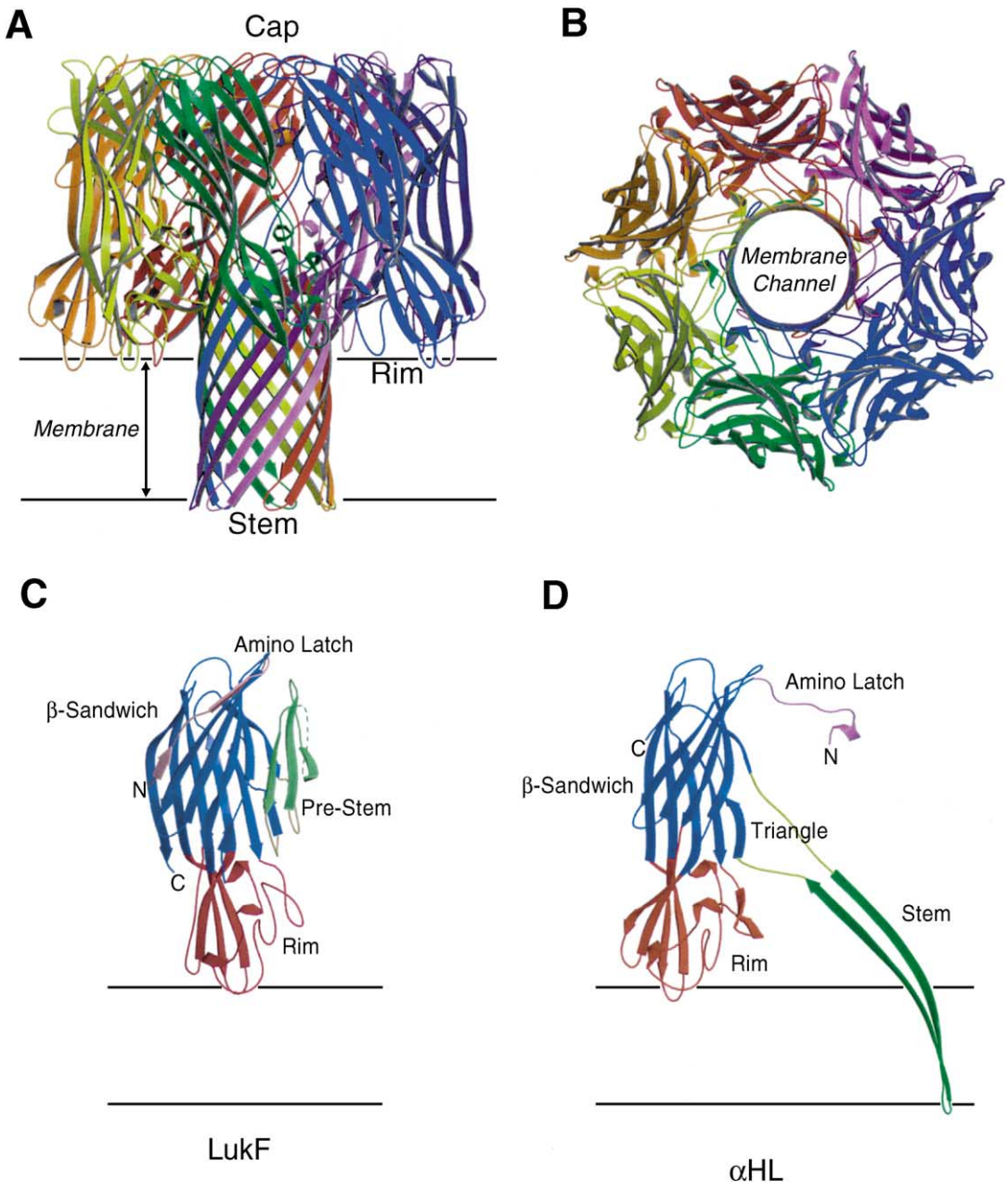

Fig. 2. Ribbon representation of the αHL heptamer viewed perpendicular to (A) and along the seven-fold axis of symmetry (B). Each protomer is a different color. The cap, rim, and stem domains are labeled. The heptamer is approximately 100 Å tall and measures 100 Å at its widest point. The channel ranges in diameter from 14 to 46 Å. The hydrophobic, transmembrane portion of the assembled pore is approximately 28 Å thick. The LukF monomer (C) and a protomer removed from the αHL heptamer (D) are shown in ribbon representation with predicted binding to the membrane and the amino latch, β-sandwich, triangle, (pre-)stem, and rim domains labeled.

class F proteins share 72% identity and their three-dimensional structures are very similar. Superposition of the structures gives a root-mean-square difference of 1.0 Å for 292 out of 301 C_α atoms, with the major deviations occurring in the loop regions and at the N and C termini [31]. The core of the secreted monomers is very similar to the αHL protomer (Fig. 2). The β sandwich is composed of 2 six-strand anti-parallel β sheets. The rim domain extends underneath the β sandwich and the orientation of the two domains with respect to each other is the same in LukF and LukF-PV. However, an 11° to 15° rotation is needed to superimpose the rim domains of a soluble monomer and an αHL protomer after superposition of the β-sandwich domains. It is not clear whether this is due to the difference in sequence or assembly state. The axis about which this rotation occurs is located at the interface between the two domains [15,16,31].

In addition to this difference in relative domain orientation, there are two striking structural differences between the αHL protomer and the soluble proteins. The amino latch,

residues 1–12 in the water-soluble LukF proteins, adopts a β conformation, adjoining the inner β sheet of the β sandwich [15,16]. In contrast, the amino latch of the αHL protomer has non-α, non-β structure with one turn of a 3_{10} helix and forms both polar and nonpolar contacts with the inner β sheet of its neighboring protomer [17]. It is possible that the amino latches of αHL and LukF have different conformations in their respective oligomers. The stem domain, which contributes two extended β strands to the transmembrane pore in αHL, has a dramatically different and compact folded conformation in the monomer structure, referred to as the prestem. This prestem domain, comprising residues 110–144 in LukF, forms a three-strand anti-parallel β sheet that packs against the β-sandwich core through hydrophobic van der Waals contacts [15]. The fold of the domain is topologically related to a family of snake venom toxins [16]. In LukF, portions of this glycine-rich region are disordered, and in the water-soluble αHL monomer, this region is protease accessible, suggesting that this domain is highly flexible in the water-soluble form of the toxin.

2. Membrane contacts

Direct rim domain interactions with the lipid headgroups of the membrane bilayer are suggested by the close proximity of the rim's base to the transmembrane region of the stem domain. Co-crystals of the αHL heptamer with diheptanoyl phosphatidylcholine demonstrate association of the lipid in the crevice between the tip of the stem domain and the rim domain [17]. A similar binding site was observed for the LukF monomer co-crystallized with dipropanoyl phosphatidylcholine [15], and the choline-like buffer MES was found associated in the same position in the LukF-PV crystal structure [16]. Fluorescence changes on binding of an acrylodan-labeled single cysteine mutant at position 266 [28] and spectroscopic probes of conformational changes in the toxin upon membrane binding and insertion [32] support the idea that the rim domain is in contact with the lipid bilayer. The surface of the rim domain of αHL has numerous solvent-exposed aromatic residues (Y68, W179, Y182, W187, W190, W260, W265, W274; see Fig. 3) [33], with six of the eight tryptophans localized to the rim surface. Intrinsic tryptophan fluorescence emission (ITFE) studies show that Trp contacts with the hydrophobic membrane environment account for increases in ITFE [34,35] for membrane-bound αHL as compared to the water-soluble monomer.

Before the αHL structure determination, Valeva et al. [28,36,37] and Ward et al. [30] had demonstrated that residues 126–140 in the stem domain participate in forming the transmembrane pore. Both ends of the stem are ringed with polar and charged residues, whereas the intervening residues form an uncharged band that lines the stem exterior. This hydrophobic belt is defined at its top by a ring of aromatic amino acids formed by Y118 and F120 (Fig. 3) and at its bottom by G126 [17]. The nonpolar belt interacts with the nonpolar portion of the bilayer, and is thick enough (~ 28 Å) to span the hydrophobic portion of the erythrocyte bilayer. On the basis of three-dimensional structures of membrane proteins and studies of transmembrane model

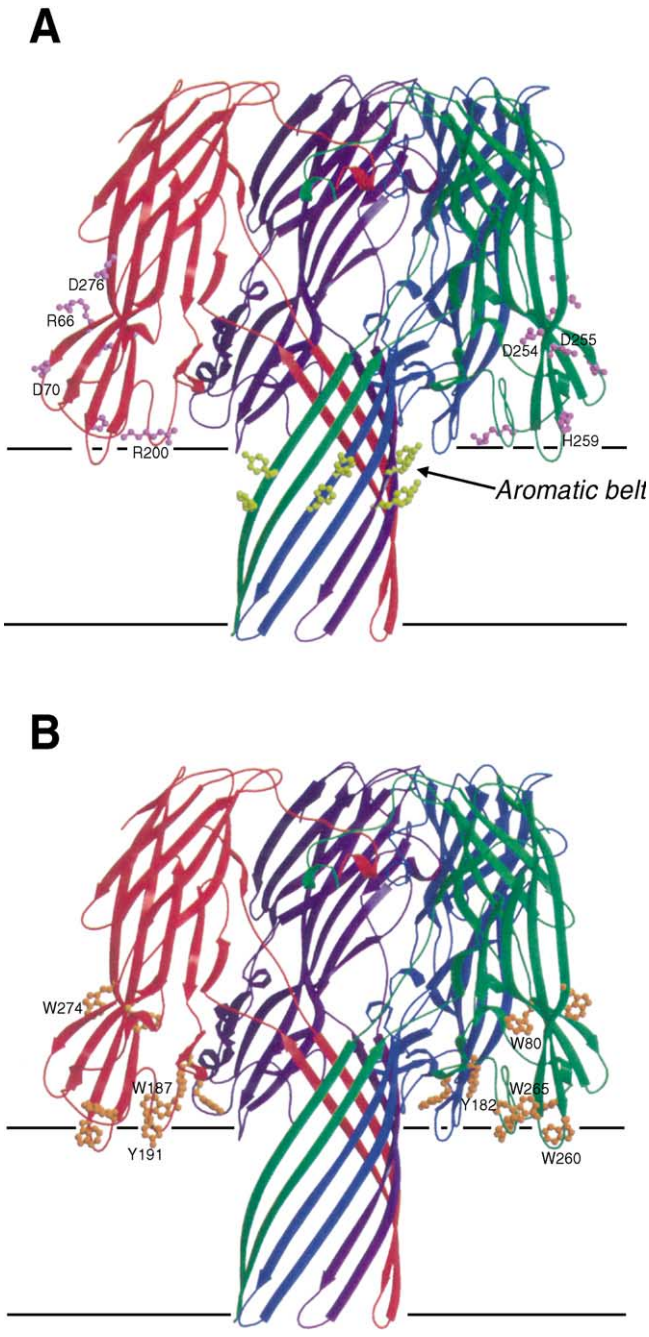

Fig. 3. Ribbon representation of four protomers from the heptamer structure, viewed perpendicular to the seven-fold axis of noncrystallographic symmetry. In (A), polar residues that have been implicated in binding [44] are shown in violet and ball-and-stick representation. The hydrophobic belt formed by residues Y118 and F120 is highlighted in yellow ball-and-stick representation. The abundance of aromatic residues found in the rim domain is illustrated in (B), with tryptophans and tyrosines drawn in orange ball-and-stick representation.

peptides, it appears that the aliphatic side chains of uncharged amino acids prefer the lipid hydrocarbon chains, the aromatic residues favor the lipid carbonyl portion of the bilayer, and the polar residues interact with the charged lipid headgroups [38]. This transmembrane residue organization is consistent with the observed arrangement of residues in the αHL pore. The interaction of distinct membrane environments with complementary transmembrane segments certainly must play an important role in folding and in defining the final position of the transmembrane pore in the perforated bilayer [39].

3. Mechanism of assembly

A wealth of biochemical and genetic data support the mechanism of αHL assembly illustrated in Fig. 4 [29,40]. αHL is secreted as a water-soluble monomer (α_1). Upon binding to the membrane of a susceptible cell, the membrane-bound monomer (α_1*) assembles to a membrane-embedded heptamer (α_7) via a nonlytic heptameric prepore (α_7*). The high affinity with which αHL binds to sensitive cells, such as rabbit erythrocytes, suggests that membrane binding is receptor mediated, but a receptor remains to be identified. The membrane-embedded heptamer creates a water-filled channel in the bilayer, leading to a disruption of the cellular chemiosmotic balance and finally, if a sufficient number of toxins pierce the bilayer, cell lysis.

The water-soluble monomer is sensitive to trypsinolysis. The two susceptible trypsin cleavage sites are at Lys8 in the N-terminal amino latch and Lys131 in the glycine-rich region. The proteolytic accessibility of the glycine-rich region coincides with an area of disorder observed in the LukF structure [15], suggesting that the prestem is flexible and solvent exposed in the water-soluble form of the toxin. An amino-terminal truncation mutant, αHL (A3–293) was accessible to proteolysis near the N terminus [29]. This mutant was retarded in the rate of oligomerization, allowing for the observation of monomeric and oligomeric states that were resistant to cleavage in the glycine-rich region when bound to the surface of a rabbit erythrocyte, and it was also deficient in pore formation. Membrane binding may occlude the proteolysis sites located in the glycine-rich loop, hindering the ability of proteolytic enzymes to cleave at these locations. Through the use of site-directed mutants that are unable to form membrane-inserted channels, it was observed that the heptameric prepore remains sensitive to trypsin at the N terminus [23] and can be dissociated to monomers by sodium dodecyl sulfate (SDS) at room temperature. In contrast, the fully assembled heptamer is SDS insensitive at temperatures up to 65 °C and is remarkably resistant to trypsin-mediated proteolysis.

A series of experiments using single-cysteine replacement mutants in conjunction with fluorescent probes has been used to study the membrane insertion event. The fluorescence studies using acrylodan-labeled cysteine mutants have shown that residues 118–140 within the glycine-rich loop move from a hydrophilic to a hydrophobic environment upon pore formation [28,36]. This transition occurs only after toxin oligomerization on membranes and corresponds to the protein inserting into the membrane. The prepore to pore transition is a cooperative process; experiments using hybrid oligomers composed of active and functionally deficient toxin monomers showed that inactive subunits were able to suppress the membrane-penetrating action of active subunits [28]. The transition from prepore to assembled heptamer may occur in a series of substates (α_7*a,b,c) [41], with evidence suggesting that intraprotomer communication between an amino latch and prestem may activate the prestem for membrane insertion, and that an

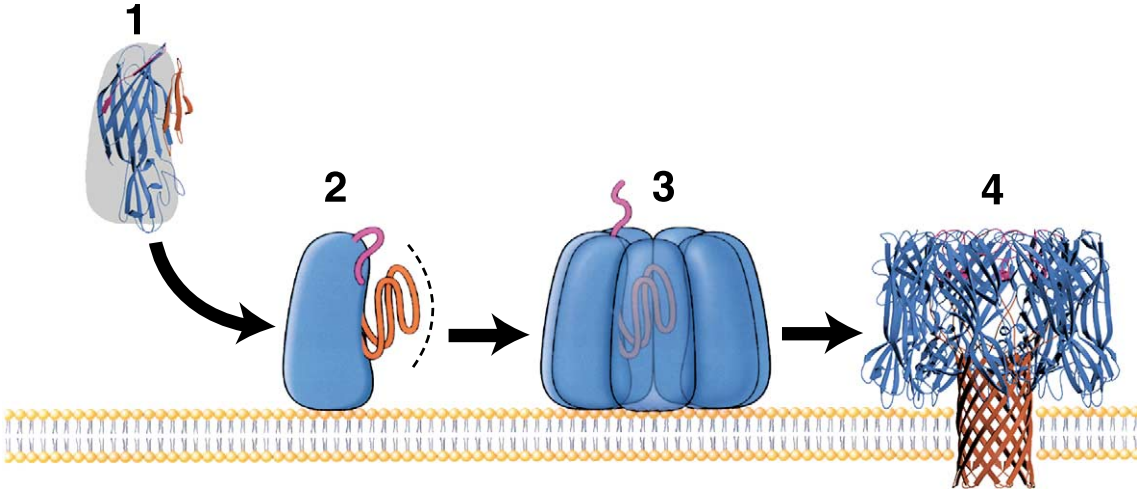

Fig. 4. Mechanism of αHL assembly. The structure for LukF (1), drawn in ribbon representation, represents the water-soluble form of the toxin. The membrane-bound monomer (2) and prepore (3) are drawn in cartoon, as their structures are unknown, although the fold of the protomer core is almost certainly preserved. The assembled heptamer (4) is drawn in ribbon representation. The protomer cores are blue and the amino latches (pink) and glycine-rich prestem (monomer and prepore states) and stem (heptamer) domains (orange) are also shown.

activated prestem may activate other prestem loops within the prepore [42]. Deletions at the N terminus [29,43] and mutations within the glycine-rich region [44,45] yielded nonlytic heptamers, indicating that these areas play important roles in the transition from heptameric prepore to assembled pore.

4. β-Barrel membrane protein folding

For membrane proteins, and particularly for β-barrel membrane proteins, progress has lagged in establishing the fundamental principles of folding and structure. Some of the better studied β-barrel membrane proteins are the outer membrane proteins (Omps) (reviewed in Ref. [46]), and the best examined of these in terms of folding mechanism is OmpA. Structural and kinetic studies performed using the transmembrane domain of OmpA [47–49] have resulted in a model for the insertion and folding of OmpA in the outer membrane. The insertion and folding reaction occurs spontaneously without the need of accessory proteins. In the aqueous phase, OmpA is unstructured and encounters the membrane in this state. Upon membrane association, a molten disc is formed, a membrane-bound intermediate localized at the interfacial region of the bilayer composed of single or paired β-strands dynamic and metastable hydrogen-bonding contacts. Subsequent to this stage, an inside-out molten globule is formed, having some of the characteristics of β-barrels. The native structure is achieved only after an extensive amount of rearrangement for proper side-chain contacts and backbone hydrogen bonding between strands [49]. The molten disc described here may be analogous to the prepore intermediate of αHL. For both proteins, the membrane insertion process is the rate-limiting step, most likely because of the side chain and secondary structure rearrangements required for pore formation. The major difference between the two assemblages lies in the fact that OmpA inserts its entire polypeptide chain into the membrane to form its pore, whereas αHL maintains a stable core structure, which is defined by the β-sandwich and rim domains, and inserts only a small portion of its seven protomers to form the transmembrane channel.

White et al. have developed a model system for examination of the thermodynamic and structural parameters of β-strand folding in the membrane [39,50–53]. Using small model peptides, they have calculated the cost of peptide bond partitioning into nonpolar phases (partitioning–folding coupling) [53]. After observing the cooperative β-sheet formation of hydrophobic peptides in lipid bilayers, they suggest that secondary structure formation is driven by hydrogen bonding, which reduces the free energy of peptide bond partitioning [52]. For αHL, which buries ~154 residues in the membrane during pore formation, the total effect on the lowering of free energy would be great, and may help explain why pore formation for the toxin is essentially irreversible. If interstrand backbone hydrogen bonds drive and stabilize β-sheet formation [50], then the side chains are left to form favorable interactions with the membrane bilayer. This supports the observed requirement for nonpolar residues in the transmembrane regions of β-barrel membrane proteins.

5. Applications

αHL has been used for a range of applications in the bioengineering field. Studies have focused on manipulating pore assembly from monomers and on manipulating properties of fully assembled pores. It has been possible to control αHL assembly using chemical, physical, and biochemical agents. Placement of a pentahistidine sequence in the glycine-rich loop creates an assembled pore with channel currents modulated by metal ions [54]. The currents can be switched 'off' by the addition of Zn^{2+}, for example, and can be turned 'on' with the addition of the zinc-chelating reagent ethylenediaminetetraacetic acid (EDTA). A protease-activated αHL was made using complementary mutagenesis [55], in which αHL proteins were produced with redundant, protease-sensitive sequences in the glycine-rich stem domain. These duplicate sequences prevented pore formation, but proteolytic removal of the redundancies activated channel insertion. Light has also been used as a trigger for pore formation. Light-sensitive sulfhydryl reagents were used to block the hemolytic activity of single-cysteine αHL mutants and hemolytic activity was restored after UV irradiation regenerated the sulfhydryl group [56].

The crystal structure of the heptamer has aided in engineering the properties of the fully assembled pore. When equipped with a noncovalently bound adapter molecule that mediates channel blocking by small molecule analytes, αHL can work as a stochastic sensor [57]. One of the adapter molecules, β-cyclodextrin (βCD), is a cyclic molecule comprised of seven D-glucose units that binds to the lumen of the assembled pore and is able to accommodate small 'guest' molecules or analytes. Because different analytes have characteristic residence times and cause a particular degree of channel blocking mediated by βCD, it is possible to detect specific analytes in a single-channel recording system. Single-stranded (ss) DNA and RNA have also been detected using single-channel conductance measurements of an αHL pore. Akeson et al. [58] used the toxin channel to analyze the composition and linear sequences within a single ssRNA polymer on the basis of channel blockade amplitude and/or residence time when the molecule is driven through the pore. By using a ssDNA polymer with an analyte-binding site as the sensor molecule, the presence of an analyte molecule can be detected through a change in DNA blockade of the channel [59]. This presents an opportunity to use multiple sensor molecules that can all bind in the toxin pore,

therefore allowing for the detection of many different types and sizes of analytes.

6. Conclusion

The application of αHL in the field of bioengineering has been demonstrated, and the biochemical and structural studies performed thus far greatly aid understanding of the mode of action of the toxin. Of even greater interest is its applicability in membrane protein-folding studies. As described earlier, the thermodynamics of OmpA membrane folding have been well examined. However, αHL may prove to be a more tenable model for understanding the mechanism of β-barrel folding in membrane bilayers. A major difficulty, which precludes a better understanding of insertion and folding in the membrane, is the ability to obtain protein in the initial, intermediate, and final steps of assembly in the membrane. As has been demonstrated experimentally and outlined here, the model for αHL assembly provides a framework to be used in studying the process of folding and insertion in the membrane. Extensive biochemical studies have identified mutants halted at intermediate stages of toxin assembly, and crystallographic studies have provided the structures of the initial and final stages in channel formation. Future structural studies, focused on the assembly intermediates, will provide snapshots of the folding pathway and provide insight into the processes involved in the assembly and folding of β-barrel proteins.

Acknowledgements

Support for the research on pore forming toxins in the Gouaux laboratory was provided by the NIH (E.G.) and by a Molecular Biophysics Training Grant (M.M.).

References

[1] P.J. Booth, A.R. Curran, Curr. Opin. Struck. Biol. 9 (1999) 115–121.
[2] R. Fussle, S. Bhakdi, A. Sziegoleit, J. Tranum-Jensen, T. Kranz, H.J. Wellensiek, J. Cell Biol. 91 (1981) 83–94.
[3] A. Zitzer, I. Walev, M. Palmer, S. Bhakdi, Med. Microbiol. Immunol. (Berl.) 184 (1995) 37–44.
[4] K. Sekiya, R. Satoh, H. Danbara, Y. Futaesaku, J. Bacteriol. 175 (1993) 5953–5961.
[5] A. Olofsson, H. Hebert, M. Thelestam, FEBS Lett. 319 (1993) 125–127.
[6] C. Petosa, R.J. Collier, K.R. Klimpel, S.H. Leppla, R.C. Liddington, Nature 385 (1997) 833–838.
[7] E.L. Benson, P.D. Huynh, A. Finkelstein, R.J. Collier, Biochemistry 37 (1998) 3941–3948.
[8] S. Bhakdi, J. Tranum-Jensen, Microbiol. Rev. 55 (1991) 733–751.
[9] T. Tomita, Y. Kamio, Biosci. Biotechnol. Biochem. 61 (1997) 565–572.
[10] E. Gouaux, M. Hobaugh, L. Song, Protein Sci. 6 (1997) 2631–2635.
[11] N. Sugawara, T. Tomita, Y. Kamio, FEBS Lett. 410 (1997) 333–337.
[12] N. Sugawara-Tomita, T. Tomita, Y. Kamio, J. Bact. 184 (2002) 4747–4756.
[13] G. Miles, L. Movileanu, H. Bayley, Protein Sci. 11 (2002) 894–902.
[14] G. Prevost, in: J.E. Alouf, J.H. Freer (Eds.), The Comprehensive Sourcebook of Bacterial Protein Toxins, Academic Press, London, 1999, pp. 402–418.
[15] R. Olson, H. Nariya, K. Yokota, Y. Kamio, E. Gouaux, Nat. Struct. Biol. 6 (1999) 134–140.
[16] J.D. Pedelacq, L. Maveyraud, G. Prevost, L. Baba-Moussa, A. Gonzalez, E. Courcelle, W. Shepard, H. Monteil, J.P. Samama, L. Mourey, Struct. Fold. Des. 7 (1999) 277–287.
[17] L. Song, M.R. Hobaugh, C. Shustak, S. Cheley, H. Bayley, J.E. Gouaux, Science 274 (1996) 1859–1866.
[18] S. Bhakdi, R. Fussle, J. Tranum-Jensen, Proc. Natl. Acad. Sci. U. S. A. 78 (1981) 5475–5479.
[19] H. Ikigai, T. Nakae, Biochem. Biophys. Res. Commun. 130 (1985) 175–181.
[20] N. Tobkes, B.A. Wallace, H. Bayley, Biochemistry 24 (1985) 1915–1920.
[21] R.J. Ward, K. Leonard, J. Struct. Biol. 109 (1992) 129–141.
[22] J.E. Gouaux, O. Braha, M.R. Hobaugh, L. Song, S. Cheley, C. Shustak, H. Bayley, Proc. Natl. Acad. Sci. U. S. A. 91 (1994) 12828–12831.
[23] B. Walker, O. Braha, S. Cheley, H. Bayley, Chem. Biol. 2 (1995) 99–105.
[24] M.S. Malghani, Y. Fang, S. Cheley, H. Bayley, J. Yang, Microsc. Res. Tech. 44 (1999) 353–356.
[25] Y. Fang, S. Cheley, H. Bayley, J. Yang, Biochemistry 36 (1997) 9518–9522.
[26] O.V. Krasilnikov, P.G. Merzlyak, L.N. Yuldasheva, C.G. Rodrigues, S. Bhakdi, A. Valeva, Mol. Microbiol. 37 (2000) 1372–1378.
[27] D.M. Czajkowsky, S. Sheng, Z. Shao, J. Mol. Biol. 276 (1998) 325–330.
[28] A. Valeva, A. Weisser, B. Walker, M. Kehoe, H. Bayley, S. Bhakdi, M. Palmer, EMBO J. 15 (1996) 1857–1864.
[29] B. Walker, M. Krishnasastry, L. Zorn, H. Bayley, J. Biol. Chem. 267 (1992) 21782–21786.
[30] R.J. Ward, M. Palmer, K. Leonard, S. Bhakdi, Biochemistry 33 (1994) 7477–7484.
[31] G. Prevost, L. Mourey, D.A. Colin, G. Menestrina, Curr. Top. Microbiol. Immunol. 257 (2001) 53–83.
[32] B. Vecsey-Semjen, C. Lesieur, R. Mollby, F.G. van der Goot, J. Biol. Chem. 272 (1997) 5709–5717.
[33] E. Gouaux, J. Struct. Biol. 121 (1998) 110–122.
[34] R.K. Bortoleto, A.H. de Oliveira, R. Ruller, R.K. Arni, R.J. Ward, Arch. Biochem. Biophys. 351 (1998) 47–52.
[35] S.M. Raja, S.S. Rawat, A. Chattopadhyay, A.K. Lala, Biophys. J. 76 (1999) 1469–1479.
[36] A. Valeva, M. Palmer, K. Hilgert, M. Kehoe, S. Bhakdi, Biochim. Biophys. Acta 1236 (1995) 213–218.
[37] A. Valeva, I. Walev, M. Pinkernell, B. Walker, H. Bayley, M. Palmer, S. Bhakdi, Proc. Natl. Acad. Sci. U. S. A. 94 (1997) 11607–11611.
[38] J.A. Killian, G. von Heijne, Trends Biochem. Sci. 25 (2000) 429–434.
[39] S.H. White, A.S. Ladokhin, S. Jayasinghe, K. Hristova, J. Biol. Chem. 276 (2001) 32395–32398.
[40] A. Valeva, J. Pongs, S. Bhakdi, M. Palmer, Biochim. Biophys. Acta 1325 (1997) 281–286.
[41] A. Valeva, M. Palmer, S. Bhakdi, Biochemistry 36 (1997) 13298–13304.
[42] A. Valeva, R. Schnabel, I. Walev, F. Boukhallouk, S. Bhakdi, M. Palmer, J. Biol. Chem. 276 (2001) 14835–14841.
[43] S. Vandana, M. Raje, M.V. Krishnasastry, J. Biol. Chem. 272 (1997) 24858–24863.
[44] B. Walker, H. Bayley, J. Biol. Chem. 270 (1995) 23065–23071.
[45] B. Walker, M. Krishnasastry, H. Bayley, J. Biol. Chem. 268 (1993) 5285–5292.

[46] S.K. Buchanan, Curr. Opin. Struck. Biol. 9 (1999) 455–461.
[47] J.H. Kleinschmidt, L.K. Tamm, Biochemistry 35 (1996) 12993–13000.
[48] T. Surrey, F. Jahnig, J. Biol. Chem. 270 (1995) 28199–28203.
[49] L.K. Tamm, A. Arora, J.H. Kleinschmidt, J. Biol. Chem. 276 (2001) 32399–32402.
[50] C.M. Bishop, W.F. Walkenhorst, W.C. Wimley, J. Mol. Biol. 309 (2001) 975–988.
[51] S.H. White, W.C. Wimley, Biochim. Biophys. Acta 1376 (1998) 339–352.
[52] W.C. Wimley, K. Hristova, A.S. Ladokhin, L. Silvestro, P.H. Axelsen, S.H. White, J. Mol. Biol. 277 (1998) 1091–1110.
[53] W.C. Wimley, S.H. White, Nat. Struct. Biol. 3 (1996) 842–848.
[54] B. Walker, J. Kasianowicz, M. Krishnasastry, H. Bayley, Protein Eng. 7 (1994) 655–662.
[55] B. Walker, H. Bayley, Protein Eng. 7 (1994) 91–97.
[56] C.Y. Chang, B. Niblack, B. Walker, H. Bayley, Chem. Biol. 2 (1995) 391–400.
[57] L.Q. Gu, O. Braha, S. Conlan, S. Cheley, H. Bayley, Nature 398 (1999) 686–690.
[58] M. Akeson, D. Branton, J.J. Kasianowicz, E. Brandin, D.W. Deamer, Biophys. J. 77 (1999) 3227–3233.
[59] J.J. Kasianowicz, S.E. Henrickson, H.H. Weetall, B. Robertson, Anal. Chem. 73 (2001) 2268–2272.